Radiation Physics and Chemistry 166 (2020) 108504

Contents lists available at ScienceDirect

Radiation Physics and Chemistry

journal homepage: www.elsevier.com/locate/radphyschem

Preparation and characterization of solution-processible polymer-grafted reduced graphene oxide by a radiation technology

Chan-Hee Jung, In-Tae Hwang, Joon-Yong Sohn, Junhwa Shin*

Radiation Research Division, Advanced Radiation Technology Institute, Korea Atomic Energy Research Institute, Jeollabuk-do, 56212, Republic of Korea

ARTICLE INFO

Keywords:
Polymer-grafted reduced graphene oxide
Graphene nanoflakes
γ-ray irradiation
Solution-processed thin film

ABSTRACT

In this research, we demonstrate that polyvinylpyrrolidone-grafted reduced graphene oxide (PVPrGO) with solution processibility can be easily produced by using a radiation technique at room temperature without any harmful reducing agent. The graphene oxide (GO) obtained from graphite flakes using a modified Hummer's method was modified through a carbodiimide-mediated coupling reaction with 4-aminostyrene to bring in polymerizable double bonds. The modified GO (MGO) was dispersed in a monomer solution of *N*-vinylpyrrolidon (NVP) in DMF, and the resulting mixtures were then irradiated with a γ-ray at room temperature to obtain a polymer grafted reduced graphene oxide (PVPrGO). The analytical results verified that PVPrGO is successfully produced via γ-ray irradiation-induced reduction of MGO and simultaneous graft polymerization of NVP, and its properties depend on the absorbed doses and monomer concentrations. Furthermore, the evaluation of the solution-processed thin film reveals that PVPrGO could provide the full-cover uniform thin film with a good electrical conductivity, overwhelming those of conventional graphene nanoflakes (GNFs).

1. Introduction

Graphene, a two-dimensional atomic layer of carbon in which the atoms are arranged in a honeycomb lattice, has skyrocketed as a hot research topic in nanotechnology since discovered by the Geim and Novoselove in 2004 owing to its extraordinary electrical, thermal, mechanical, and optical properties (Allen et al., 2010; Geim and Novoselov, 2007; Novoselov et al., 2004; Singh et al. 2011). Taking into consideration the productivity and cost, a graphene oxide (GO)-reduction strategy has seemed to be the most promising method thus far (Chua and Pumera 2014). However, a graphene nanoflakes (GNFs) produced through the graphene oxide (GO)-reduction has exhibited poor dispersibility in common solvents owing to a π-π stacking-induced irreversible agglomeration limiting their diverse applications (Stankovich et al., 2007; Li et al., 2008).

To improve the dispersibility, functionalization of GNFs has been widely investigated through a non-covalent and covalent modification of GO and a post reduction (Chua and Pumera 2013; Wang et al., 2015). Among them, a covalent polymer-grafting strategy has been most preferred over the others owing to the covalently-grafted long polymer chains allowing a high dispersibility of functionalized GNFs in a wide range of solvents even at a low degree of functionalization (Layek and Nandi, 2013). Generally, the polymer-grafted GNFs have been developed mainly through polymer grafting of GO and a chemical reduction based on living radical polymerization (Bardi et al. 2012), free radical polymerization (Backert et al. 2013), condensation polymerization (Xue et al., 2015), coupling reaction with polymer (Yadav et al., 2012), or many others (Dinda et al., 2013). On the other hand, these proposed strategies have several drawbacks including multi-step functionalization and a reduction process, the necessity of toxic and explosive additives, and high temperature, and low productivity (Tran et al., 2014; Pham et al., 2011; Thakur and Karak, 2015). Therefore, the cost-effective and scalable strategy for the highly-dispersible GNFs has been highly demanded for the mass production.

A radiation-based technique could provide a promising way to prepare highly-dispersible polymer-grafted GNFs. This technique offers several advantages including room-temperature chemical reactions of graft polymerization and reduction without toxic additives of initiator and reducing agent, easy control of the chemical reaction, and large scalability (Chen et al., 2012; Gupta et al. 2016; Jung et al., 2017). Despite these discriminable merits, the synthesis of polymer-grafted reduced graphene oxide though a radiation-based technique has been rarely studied to produce highly-dispersible GNFs (Chen et al., 2012; Feng et al., 2012; Jung et al., 2017).

This research was aimed to prepare a solution-processible polyvinylpyrrolidone-grafted reduced graphene oxide (PVPrGO) by using a

* Corresponding author.
E-mail address: shinj@kaeri.re.kr (J. Shin).

https://doi.org/10.1016/j.radphyschem.2019.108504
Received 25 July 2019; Received in revised form 30 August 2019; Accepted 25 September 2019
Available online 06 October 2019
0969-806X/

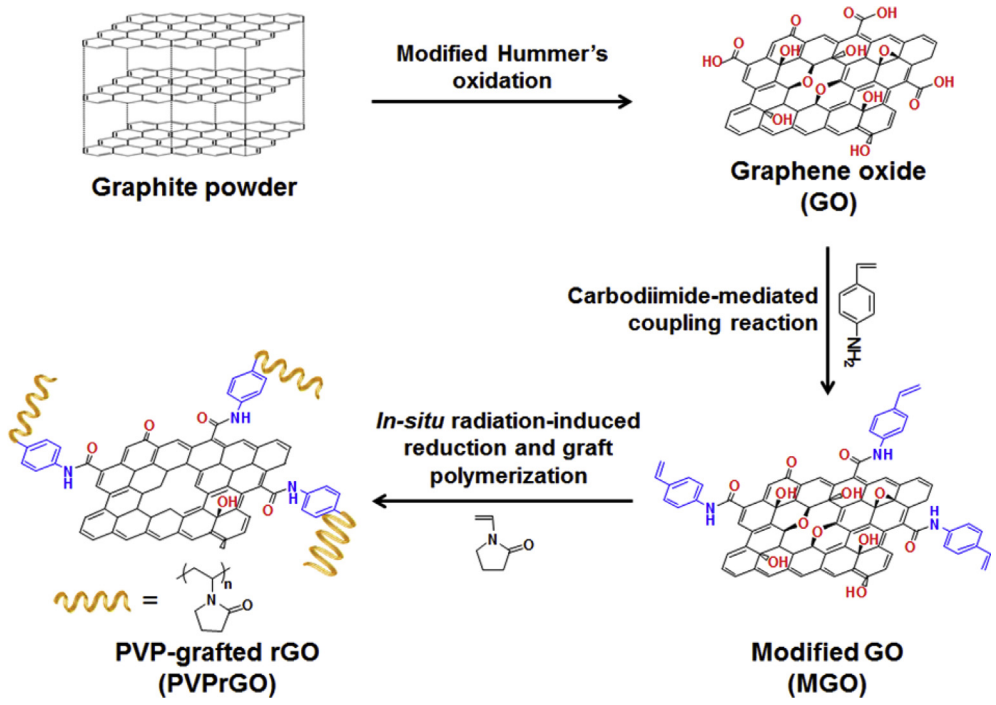

Fig. 1. Schematic diagram for the preparation of PVPrGOs.

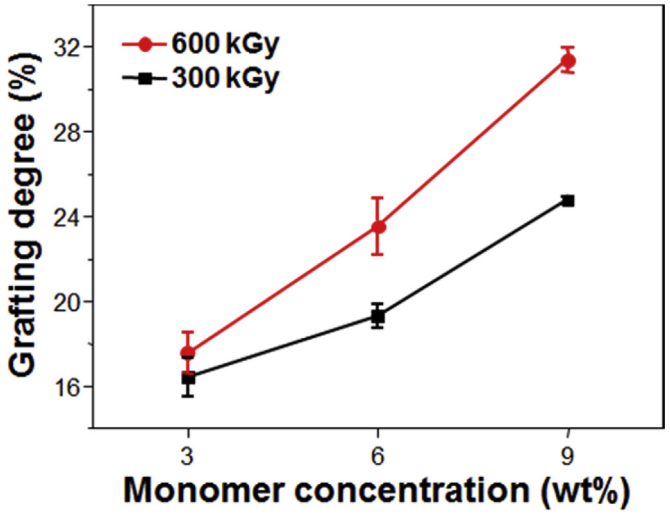

Fig. 2. Grafting degree of PVPrGOs with a monomer concentration and absorbed dose.

reducing agent-free and room-temperature radiation technique. For this, the modified GO (MGO) was synthesized through a carbodiimide-mediated coupling reaction of GO with 4-aminostyrene. To figure out the formation of PVPrGO, *in-situ* reaction of γ-ray irradiation-induced reduction and graft polymerization with different concentration of MGO and monomer solution was performed under two absorbed doses and different monomer concentrations. The resulting PVPrGO was systematically characterized by using analytical techniques including grafting degree measurements, UV–Vis (ultraviolet–visible spectroscopy), Fourier transform infrared spectroscopy (FT-IR), X-ray photoelectron spectroscopy (XPS), Raman spectroscopy, XRD (X-ray diffraction), and dispersion tests. Furthermore, the electrical properties of its thin film were investigated to evaluate its solution processability.

2. Experiments

2.1. Materials

Graphite powder (SP-1, Bay carbon) was used in the preparation of GO. 4-Aminostyrene (Tokyo Chemical Industry Company, ≥ 95% purity) and *N,N′*-diisopropylcarbodiimide (DIC, 99% purity, Aldrich) were utilized in the preparation of MGO. *N*-vinylpyrrolidone (NVP, ≥ 99% purity, Aldrich) and *N,N′*-dimethylformamide (DMF, 99.8% purity, Aldrich) were employed in the preparation of PVPrGO. Potassium hydroxide (KOH, ≥ 85% purity, Showa) and ethanol (EtOH, 99.8% purity, Showa) were used in the cleavage reaction. Tetrahydrofuran (THF, 99.5% purity, Showa) was employed in the dispersion stability test. All chemicals in this research were used as received.

2.2. Preparation of MGO

GO was prepared from graphite powder using a modified Hummer's method (Tung et al., 2009). The MGO was prepared according to the procedure reported in the previous work (Jung et al., 2017). Briefly, 0.5 g of GO was well dispersed in 100 mL of DMF solvent through ultrasonication for 30 min. 7.5 g of DIC was added into the GO solution and the mixture stirred for 1 h. Afterwards, 2 g of aminostryene solution in 5 mL of DMF was poured into the mixture solution, and then the mixture stirred for 24 h at room temperature. The MGO was then obtained by filtrating with 0.2 μm PTFE membrane filter (Millipore), washing with DMF and ethanol at least three times, and finally drying in a vacuum oven for 24 h.

2.3. Preparation of PVPrGO

0.5 g of as-prepared MGO was dispersed in 400 mL of DMF, followed by the addition of certain amounts of *N*-vinylpyrrolidone (NVP) to have a concentration of NVP ranging from 3 to 9 wt%. The homogenous mixture solution was put into glass tube, sealed with rubber septa, and finally deoxygenated with nitrogen gas purging for 30 min. To initiate the *in-situ* graft polymerization and reduction, the tubes were exposed

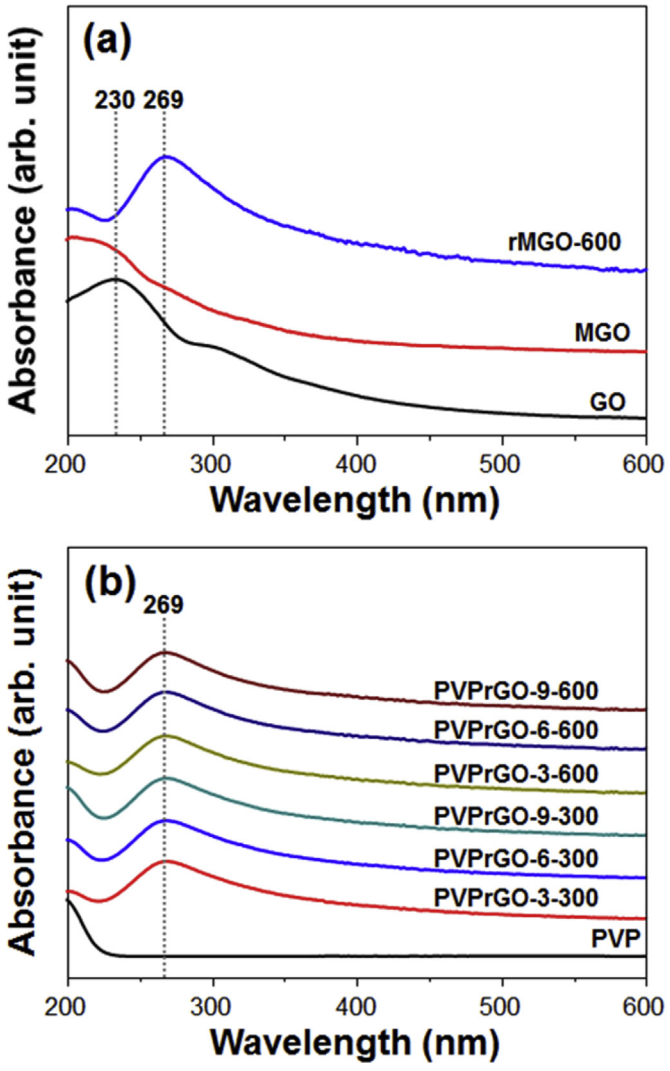

Fig. 3. UV–Vis spectra of GO, MGO, rMGO, and PVPrGOs: (a) GO, MGO, and rMGO and (b) PVP and PVPrGOs prepared at different monomer concentrations and absorbed doses.

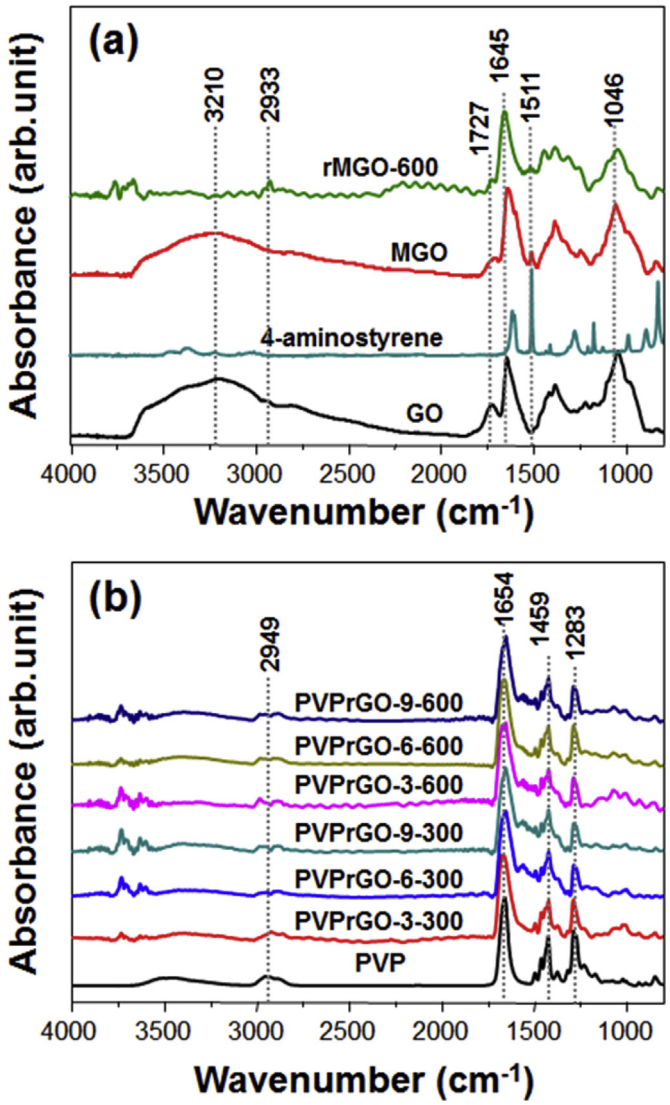

Fig. 4. ATR-FTIR spectra of GO, 4-aminostyrene, MGO, rMGO, and PVPrGOs: (a) GO, 4-aminostyrene, MGO, and rMGO and (b) PVP and PVPrGOs prepared at different monomer concentrations and absorbed doses.

to γ-ray from a ^{60}Co source at the Advanced Radiation Technology Institute (ARTI) of the Korea Atomic Energy Research Institute (KAERI). The dosimetry was carried out by using alanine dosimeters (5 mm diameter, Buker BioSpin, Rheinstetten, Germany). According to ISO/ASTM 51261 standard, the alanine dosimeter reader was calibrated with standard references supplied by the UK national physics laboratory. The studied absorbed doses were 300 and 600 kGy at a dose rate of 10 kGy/h. Afterwards, The PVPrGOs was then separated by filtrating with 0.2 μm PTFE membrane filter (Millipore), washed with DMF and ethanol at least three times, and finally dried in a vacuum oven at 50 °C at a residual pressure of 1×10^{-3} mbar for 48 h. The prepared PVPrGOs were designated as PVPrGO-X-Y where X and Y indicate the monomer concentration and absorbed dose, respectively. Furthermore, the reduced MGO (rMGO) for the comparison with PVPrGO was prepared through a γ-ray irradiation on MGO solution in DMF without monomer at an absorbed dose of 600 kGy.

2.4. Characterization

The degree of grafting was determined by weighing the mass of PVPrGOs before and after the cleavage reaction. Typically, the PVPrGO powder (100 mg) was dispersed in 30 mL of 75% aqueous ethanol solution containing 1.5 M KOH. The suspension mixture was refluxed at 70 °C for 72 h. After this cleavage reaction, the resulting reduced graphene oxide was then collected by filtration with a 0.2 μm PTFE membrane filter and then further purified through re-dispersion in deionized water and subsequent filtration at least three times to completely remove the PVP and salts solubilized in deionized water. The resulting cleaved PVPrGO was dried in a vacuum oven at 50 °C for 48 h. The grafting degree (GD) is determined by GD = $(W_0–W)/W \times 100$, where W_0 and W represent the completely dried weight of PVPrGO before and after the cleavage reaction, respectively. Ultraviolet–visible (UV–vis), Fourier transform infrared (FT-IR), X-ray photoelectron spectroscopy (XPS) spectra were recorded on a Scinco S-3100 spectrophotometer, an attenuated total reflectance Fourier transform infrared spectroscope (ATR-FTIR, Varian 640, Australia), and a MultiLab 2000 x-ray photoelectron spectroscope (Thermo Electron Corporation, England), respectively. Raman spectroscopy was performed using Raman spectrometer (LabRam-HR JobinYvon LabRAM system, Horiba Scientific). X-ray diffraction (XRD) patterns were obtained using an X-ray diffractometer (X'Pert Pro, PANlytical, Netherlands) within the 2θ range of 1° to 50°. Dispersion in water was measured by plotting the UV–Vis absorbance at 269 nm versus concentration (0.02, 0.025, 0.03, and 0.04 mg/mL), and the dispersion stability test was carried out by monitoring the precipitation of the PVPrGO-9-600 and rMGO-600 in

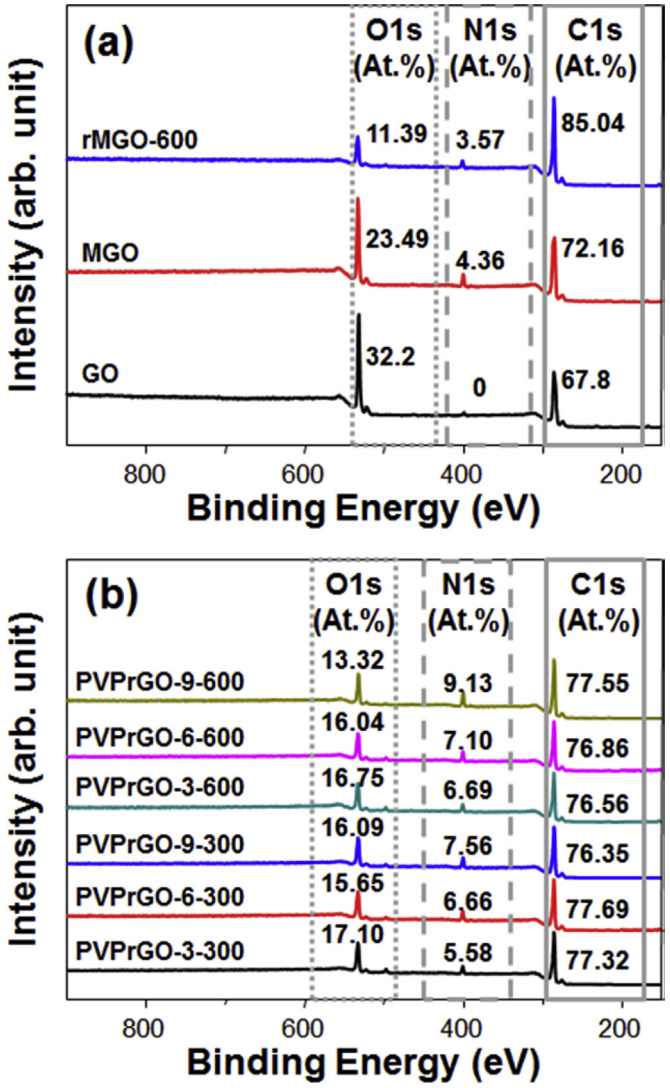

Fig. 5. XPS survey spectra of GO, MGO, rMGO, and PVPrGOs: (a) GO, MGO, and rMGO, and (b) PVPrGOs prepared at different monomer concentrations and absorbed doses.

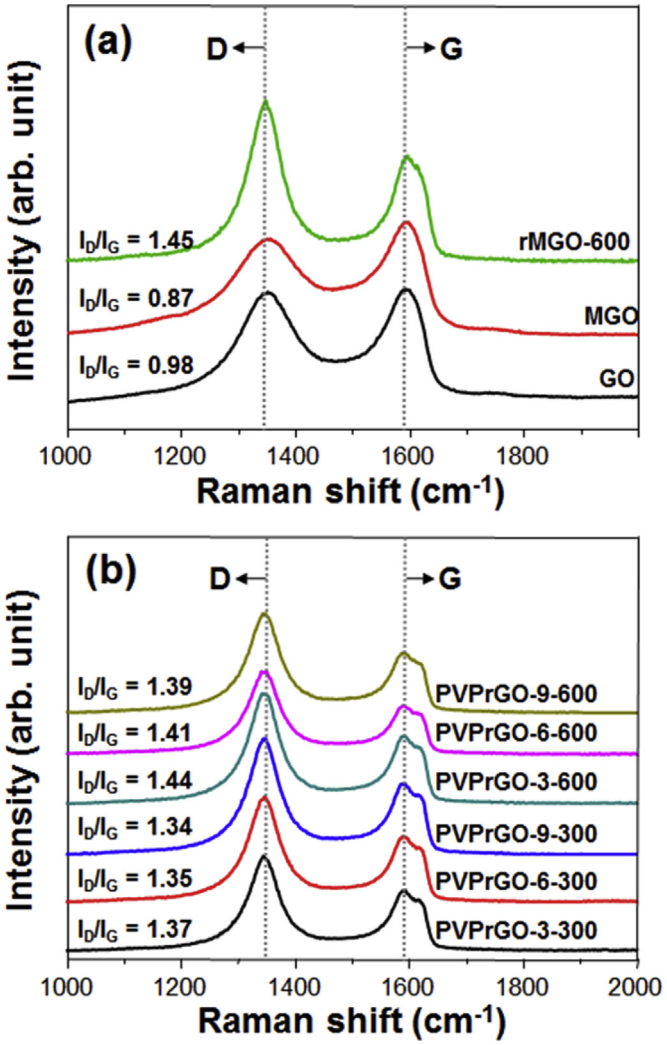

Fig. 6. Raman spectra of GO, MGO, rMGO, and PVPrGOs: (a) GO, MGO, and rMGO and (b) PVPrGOs prepared at different monomer concentrations and absorbed doses.

various solvents including DMF, EtOH, THF, and deionized water at a fixed concentration of 2 mg/mL. The electrical conductivities, transmittance, and morphology of 10 nm thick thin film on quartz measured with an AlphaStep IQ surface profiler (KLA Tencor, USA) were analyzed using a four-point probe conductivity meter (Advanced Instrument Technology, CMT, SR100N), UV–vis, and an atomic force microscope (AFM, Surface Imaging System GmbH, Germany), respectively.

3. Results and discussion

To investigate the graft polymerization during the γ-ray irradiation, the grafting degree of PVPrGO prepared according to the scheme depicted in Fig. 1 was determined by measuring the weight of PVPrGOs before and after the cleavage reaction of PVP chains from the PVPrGOs on the basis of the base-catalyzed hydrolysis of the amide bond (Gassman et al., 1976). As shown in Fig. 2, the PVPrGO showed the grafting degree ranging from 16 to 31 wt% in the given absorbed doses and monomer concentrations. This result reveals that the graft polymerization successfully occurred at the given condition and the grafting degree of polymer existing in the PVPrGO depended on the absorbed dose and monomer concentration.

To verify the formation of reduced graphene oxide in PVPrGOs, UV–Vis spectroscopy was performed, and the results are shown in Fig. 3. As shown in Fig. 3(a), the UV–vis absorption spectra of GO and MGO exhibited the identical maximum absorption peaks at 230 nm attributed to π → π* transitions of conjugated double bonds (Paredes et al., 2008). In the rMGO spectrum, the peak corresponding to π → π* transitions of conjugated double bonds was observed at a longer wavelength of 269 nm than GO and FGO. This result indicates that MGO was effective reduced by the active electrons from the radiolysis of DMF solvent during the γ-ray irradiation (Zhang et al., 2012). Likewise, all the PVPrGOs exhibited the same peaks at 269 nm, indicative of the formation of reduced graphene oxide as shown in Fig. 3(b). Therefore, PVPrGO was successfully reduced during the γ-ray irradiation.

To investigate the formation of PVPrGO from GO, an ATR-FTIR analysis was carried out, and the results are shown in Fig. 4. As displayed in Fig. 4(a), GO spectrum exhibited the characteristic peaks at 3210 cm^{-1} (O–H from GO and/or water), 1727 cm^{-1} (C═O), 1645 cm^{-1} (conjugated C═C), and 1046 cm^{-1} (C–O), respectively (Mungse and Khatri, 2014). In the MGO spectrum, the peak corresponding to the C═O bond of COOH almost disappeared at 1729 cm^{-1} and a new peak corresponding to the aromatic C═C bond of styryl group newly appeared at 1511 cm^{-1}, implying the successful covalent modification of GO with 4-aminostyrene (Remyamol et al., 2013). In comparison to MGO, rMGO spectrum exhibited a significant reduction in the peak intensities of the OH group. On the other hand, as shown in

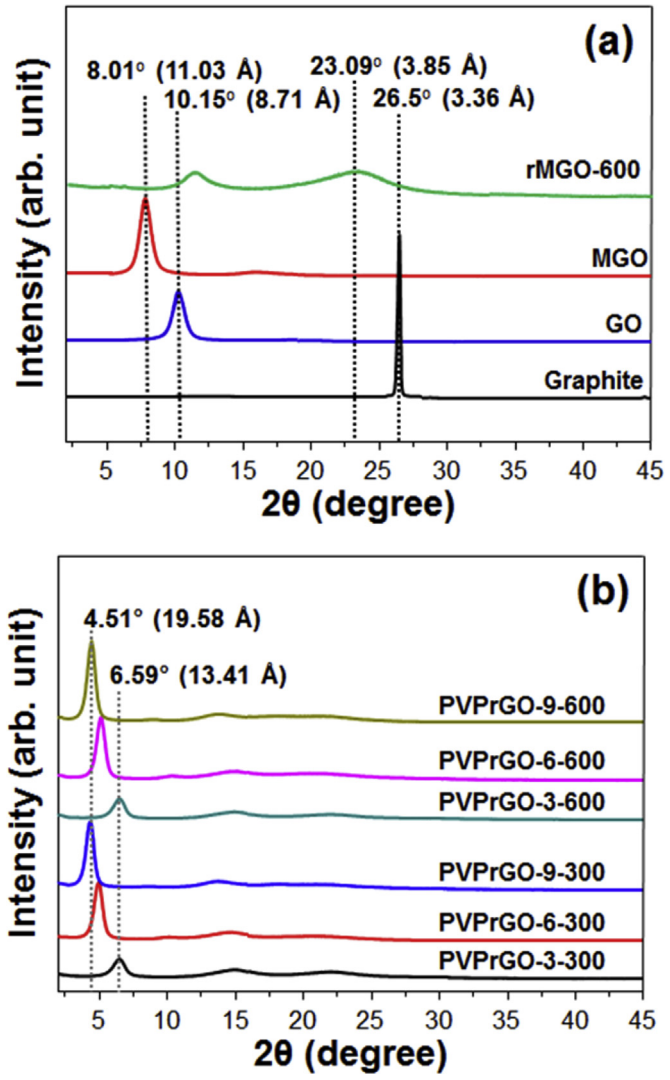

Fig. 7. XRD patterns of graphite, GO, MGO, rMGO, and PVPrGOs: (a) GO, MGO, and rMGO and (b) PVPrGOs prepared at different monomer concentrations and absorbed doses.

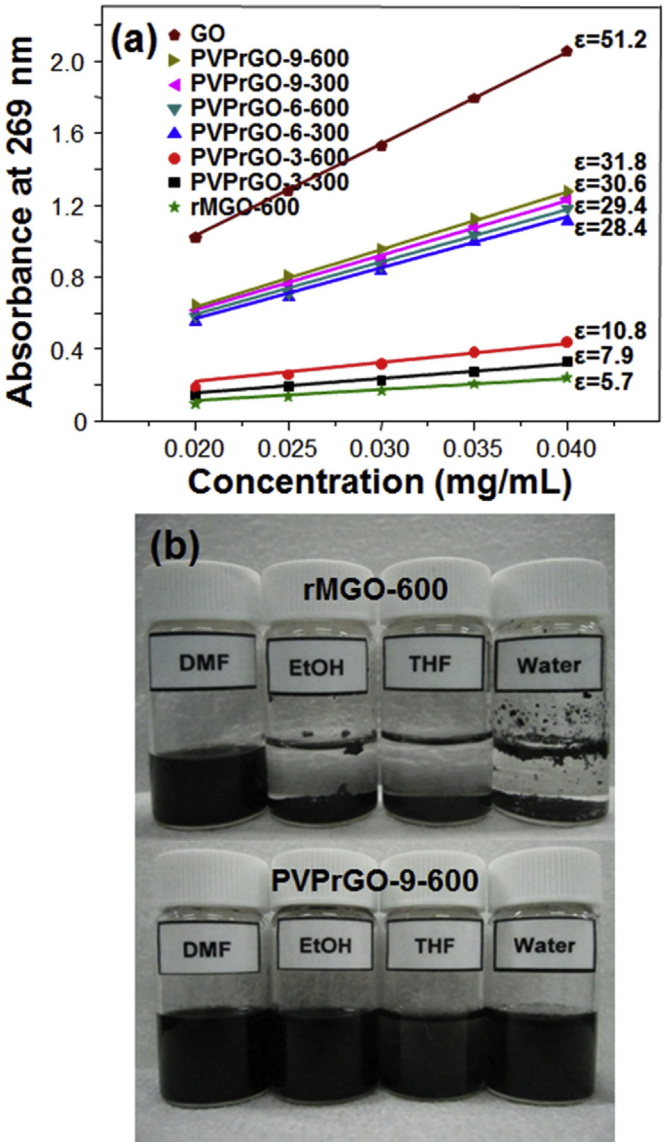

Fig. 8. (a) UV–vis absorption (at 269 nm) of GO, rMGO, and PVPrGOs prepared at different absorbed dose and monomer concentration. (b) Photo-images for dispersion of rMGO and PVPrGO-9-600 in different solvents at a concentration of 2 mg/mL after ambient storage for 3 months.

the PVPrGO spectra (Fig. 4(b)), the characteristic peaks corresponding to the chemical structure of PVP was clearly observed at 2949 cm^{-1} (C–H), 1654 cm^{-1} (N–C═O), 1459 cm^{-1} (CH_2), and 1283 cm^{-1} (C–N), respectively, and the intensities of its OH groups were evidently reduced, implying the occurrence of the reduction reaction during the irradiation like the rMGO spectrum (Feng et al., 2012). From this result, it was confirmed that PVPrGOs were successfully prepared by *in-situ* γ-ray irradiation-induced reduction and graft polymerization in the presence of NVP and MGO.

In the conjunction of FT-IR, an XPS analysis was employed to further elucidate the change in chemical composition for the formation of PVPrGO from GO through the sequential reaction. As shown in Fig. 5(a), the GO spectrum showed two elemental peaks for carbon (C) at 285 eV and oxygen (O) at 531 eV, and their contents are 67.8 at% and 32.2 at%, respectively. In the MGO spectrum, in addition to the C (72.16 at%) and O (23.49 at%) peak, a nitrogen (N) peak (4.36 at%) newly appeared at 399 eV in comparison to that of GO, indicating the successful modification of GO with 4-aminostyrene via an amide linkage. The rMGO spectrum exhibited a higher C (85.04 at%), lower O (11.39 at%), and similar N contents (3.57 at%) in comparison to that of MGO, clearly verifying the effective reduction of MGO by γ-ray irradiation (Bhangare et al., 2018; Feng et al., 2012). In contrast, as shown in the spectrum of PVPrGOs (Fig. 5(b)), the respective C and N atomic percentages were increased up to 77.6 at% and 9.1 at% with an absorbed dose and monomer concentration in comparison to those in the MGO spectrum, while the O one was decreased to 13.3 at% similar to that of rMGO. Therefore, it is reconfirmed from the XPS result that PVPrGOs were successfully produced through a γ-ray irradiation-induced simultaneous reduction of MGO and graft polymerization of NVP as mentioned in the FT-IR analysis.

The structural investigation on the formation of PVPrGO from GO through the sequential reaction was performed via Raman spectroscopy, and the results are presented in Fig. 6. As shown in Fig. 6(a), the typical characteristic G and D peaks corresponding to the sp^2-hybridized crystalline and sp^3-hybridized amorphous carbon (Sobon et al., 2012) were identically observed at 1604 and 1350 cm^{-1}, respectively, in both the GO and MGO spectra, and the D band to the G band intensity ratio (I_D/I_G) was almost similar, inferring no further formation of defects in GO induced by the covalent modification (Lomeda et al., 2008; Pham et al., 2011). In the rMGO spectrum, the D and G peaks were similar to that of MGO, but the I_D/I_G value of 1.45 was much higher than that of MGO (0.87) owing to the further increase in the

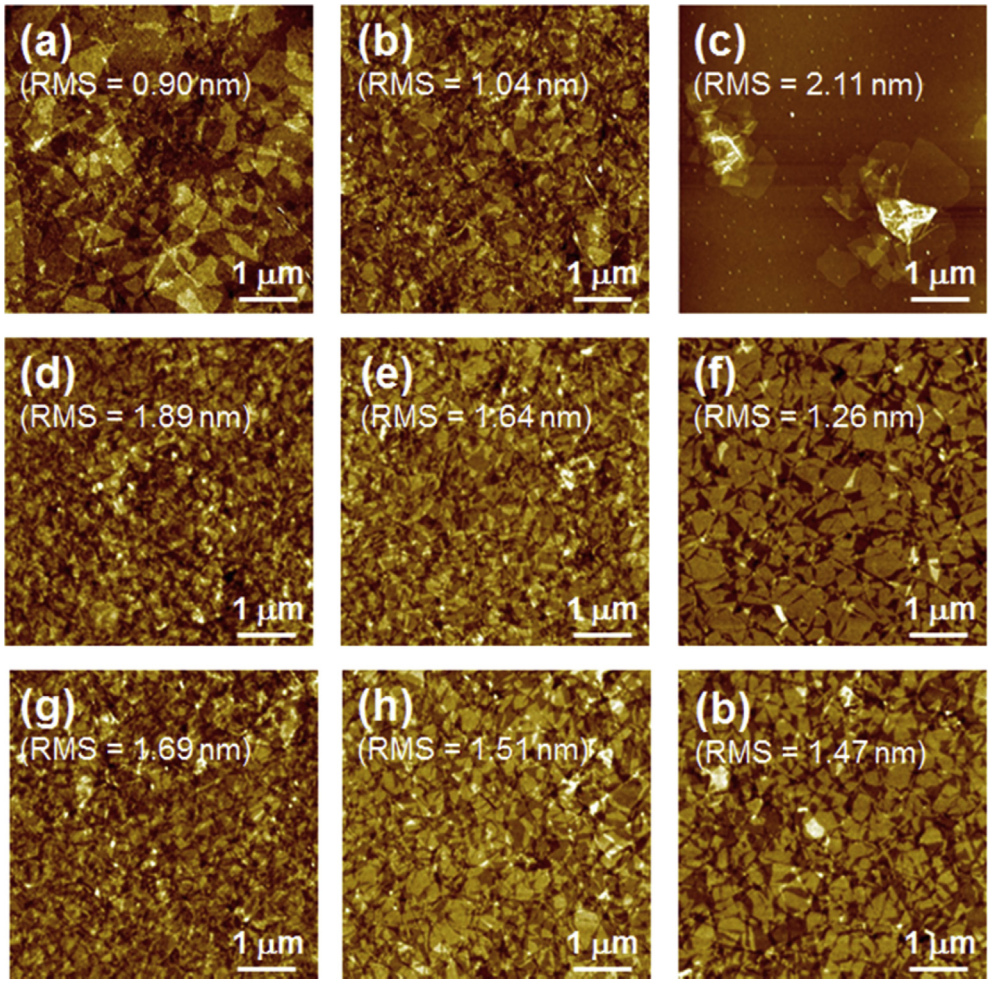

Fig. 9. AFM images of GO, MGO, rMGO and PVPrGOs films spin coated on Si-wafer: (a) GO, (b) MGO, (c) rMGO-600, (d) PVPrGO-3-300, (e) PVPrGO-6-300, (f) PVPrGO-9-300, (g) PVPrGO-3-600, (h) PVPrGO-6-600, and (i) PVPrGO-9-600.

numbers of small carbon crystal domain as reported in the literature (Pham et al., 2011). Similarly, the I_D/I_G ratios of the PVPrGOs were also increased to 1.44 with an increasing absorbed dose but almost identical with an increasing monomer concentration as shown in Fig. 6(b). This result indicates that the graft polymerization took place primarily at the introduced double bonds of the MGO; otherwise, the I_D/I_G could be much more increased because of the more formation of the disorder structure induced by the direct graft polymerization at the in-plane region of MGO described in the literature (Wang et al., 2016). From this result, it is deduced that the NVP was simultaneously graft-polymerized primarily at the introduced double bonds of MGO with a simultaneous reduction, and thereby producing PVPrGO.

To give an insight into the exfoliation extent of PVPrGO, XRD analysis was performed and the results are shown in Fig. 7. As shown in Fig. 7(a), the GO pattern shows broader peaks at 2θ of 10.15° (interlayer spacing distance (d) = 8.71 Å) in comparison to that of graphite (interlayer spacing distance (d) = 3.36 Å), meaning full exfoliation of GO. In the MGO pattern, a similar peak was presented at a slightly lower 2θ of 8.01° (corresponding to a d of 11.03 Å) than GO, indicating more exfoliation of MGO prepared by with 4-aminostyrene (Rani et al., 2014). Unlike MGO, the rMGO pattern exhibited a typical broad peak at a 2θ of 23.09° (d = 3.85 Å) originating from its irreversible interlayer π-π restacking as reported in the literature (Jung et al., 2017). On the other hand, all the PVPrGO patterns showed broad peaks at lower 2θ regions ranging from 6.59° to 4.51° in comparison to MGO (Fig. 7(b)). Therefore, this result indicates that the grafted PVP expanded the interlayer distances of PVPrGO.

To estimate the dispersibility and dispersion stability of PVPrGOs, two critical factors for the solution processing, measuring absorbance at 269 nm in relation to concentration using UV–vis and storing dispersion in different solvents of DMF, EtOH, THF, and water for 3 months were performed. As shown in Fig. 8(a), the absorbance of all suspensions was linearly increased with a concentration increase under the given concentration in accordance with the Beer-Lambert law (Chabot et al., 2013). In comparison to that of GO, rMGO exhibited an extremely lower calculated extinction coefficient (ε) of 5.7 mL/mg·cm, indicating its poor dispersion in water due to the high hydrophobicity. In contrast, although lower than that of GO, PVPrGOs exhibited a much higher ε ranging from 7.9 to 31.8 mL/mg·cm than rMGO, depending on the grafting degree. Furthermore, as shown in Fig. 8(b), the dispersions of PVPrGO-9-600 at the concentration of 2 mg/mL in all given solvents were clearly stable even after the ambient storage of 3 months. From these results, it is believed that the PVPrGOs have a greater dispersibility in common solvents than rMGO due to the existence of the grafted PVP even though they were effectively reduced (Yoo et al., 2014).

To demonstrate the solution processability, thin films of PVPrGOs on transparent quartz substrates were investigated in terms of morphology, optical transmittance, and electrical conductivity. As shown in Fig. 9(a)-(b), GO and MGO both showed identical homogenous full-covered thin films with a respective root-mean-square (RMS) roughness of 0.90 nm and 1.04 nm similar to the level (0.860 nm) of as reported in the literature, but rMGO exhibited an unevenly-covered thin film with an RMS roughness of 2.11 nm (Chen et al., 2014). On the other hand, as

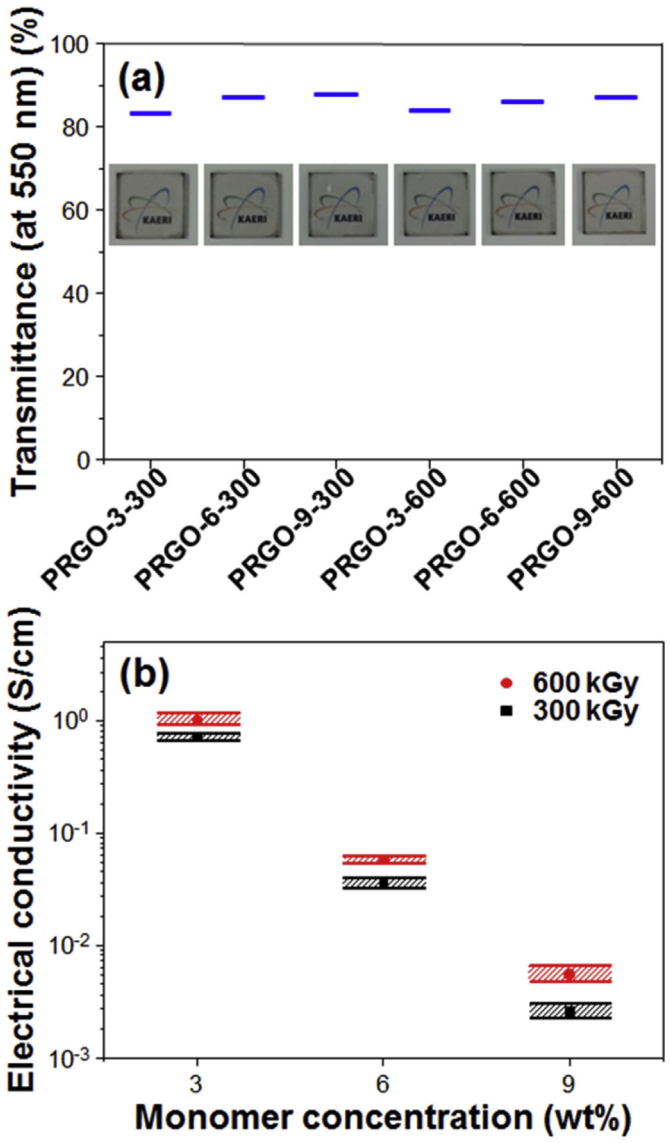

Fig. 10. Transmittance at 550 nm and electrical conductivities of PVPrGOs thin films: (a) transmittance of PVPrGOs and (b) electrical conductivities of PVPrGOs prepared at different monomer concentrations and absorbed doses.

shown in Fig. 9(d)-(i), all the PVPrGOs showed a homogeneous full-coverage thin film with an RMS roughness below 1.89 nm, indicating that, despite their effective reduction, all the PVPrGOs have a uniform thin-film formability as good as that of GO and MGO. Furthermore, as shown in Fig. 10, thin films of PVPrGO exhibited almost similar transmittances of above 84% and electrical conductivities ranging from 0.003 to 0.95 S/cm. Accordingly, it is clearly ascertained from these results that PVPrGOs can be obtained as electrically-conductive uniform thin films using a simple and low-cost solution processing favorable for the further applications.

4. Conclusions

Preparation of PVPrGOs from GO through a carbodiimide-mediated coupling reaction to introduce double bond followed by *in-situ* radiation-induced reduction and graft polymerization was successfully demonstrated in this research. The grafting degree varied from 17% to 31% with a change in the absorbed dose and monomer concentration. From the characterization results of UV–vis, ATR-FTIR, XPS, Raman, XRD, and AFM, it was confirmed that the polymerizable double bond is manifestly introduced at the COOH of GO, and PVPrGOs are successfully synthesized via the reduction of MGO with a simultaneous graft polymerization of NVP at the double bonds during the irradiation. The PVPrGOs exhibited the good long-term dispersion in aqueous solvent even at 2 mg/mL and homogenous thin-film formability. Furthermore, the electric conductivity of PVPrGOs thin film varied from 0.003 to 0.95 S/cm which was dependent on the absorbed dose and monomer concentration. Therefore, it is strongly suggested from the overall results that this radiation technology can be used in the preparation of solution-processible graphene for the electronic and biological applications.

Acknowledgement

This work was supported by the Basic Research Program of the Korea Atomic Energy Research Institute Grant funded by the Korean government.

References

Allen, M.J., Tung, V.C., Kaner, R.B., 2010. Honeycomb carbon: a review of graphene. Chem. Rev. 110, 132–145.
Backert, F., Rostas, A.M., Thomann, R., Weber, S., Schleicher, E., Friedrich, C., Mülhaupt, R., 2013. Self-initiated free radical grafting of styrene homo- and copolymers onto functionalized graphene. Macromolecules 46, 5488–5496.
Bardi, A., Whittaker, M.R., Zetterlund, P.B., 2012. Modification of graphene/graphene oxide with polymer brushes using controlled/living radical polymerization. J. Polym. Sci., Part A: Polym. Chem. 50, 2981–2992.
Bhangare, B., Jagtap, S., Ramgir, N., Waichal, R., Muthe, K.P., Gupta, S.K., Gadkari, S.C., Aswal, D.K., Gosavi, S., 2018. Evaluation of humidity sensor based on PVP-RGO nanocomposites. IEEE Sens. J. 18, 9097–9104.
Chabot, V., Kim, B., Sloper, B., Tzoganakis, C., Yu, A., 2013. High yield production and purification of few layer graphene by gum Arabic assisted physical sonication. Sci. Rep. 3, 1378.
Chen, L., Xu, Z., Li, J., Li, Y., Shan, M., Wang, C., Wang, Z., Guo, Q., Liu, L., Chen, G., Qian, X., 2012. A facile strategy to prepare functionalized graphene via intercalation, grafting and self-exfoliation of graphene oxide. J. Mater. Chem. 22, 13460–13463.
Chen, L., Du, D., Sun, K., Hou, J., Ouyang, J., 2014. Improved Efficiency and stability of polymer solar cells utilizing two-dimensional reduced graphene oxide: graphene oxide nanocomposites as hole-collection material. ACS Appl. Mater. Interfaces 6, 22334–22342.
Chua, C.K., Pumera, M., 2013. Covalent chemistry on graphene. Chem. Soc. Rev. 42, 3222–3233.
Chua, C.K., Pumera, M., 2014. Chemical reduction of graphene oxide: asynthetic chemistry viewpoint. Chem. Soc. Rev. 43, 291–312.
Dinda, D., Gupta, A., Saha, S.K., 2013. Removal of toxic Cr (VI) by UV-active functionalized graphene oxide for water purification. J. Mater. Chem. A. 1, 11221–11228.
Feng, R., Zhou, W., Guan, G., Li, C., Zhang, D., Xiao, Y., Zheng, L., Zhu, W., 2012. Surface decoration of graphene by grafting polymerization using graphene oxide as the initiator. J. Mater. Chem. 22, 3982–3989.
Gassman, P.G., Hodgson, P.K.G., Balchunis, R.J., 1976. Base-promoted hydrolysis of amides at ambient temperatures. J. Am. Chem. Soc. 98, 1275–1276.
Geim, A.K., Novoselov, K.S., 2007. The rise of graphene. Nat. Mater. 6, 183–191.
Gupta, B., Kumar, N., Panda, K., Melvin, A.A., Joshi, S., Dash, S., Tyagi, A.K., 2016. Effective noncovalent functionalization of poly(ethylene glycol) to reduced graphene oxide nanosheets through γ-radiolysis for enhanced lubrication. J. Phys. Chem. 120, 2139–2148.
Jung, C.-H., Noh, Y.-J., Bae, J.-H., Yu, J.-H., Hwang, I.-T., Shin, J.H., Shin, K.W., Lee, J.-S., Choi, J.-H., Na, S.-I., 2017. Polyacrylonitrile-grafted reduced graphene oxide hybrid: an all-round and efficient hole-extraction material for organic and inorganic-organic hybrid photovoltaics. Nano Energy 31, 19–27.
Layek, R.K., Nandi, A.K., 2013. A review on synthesis and properties of polymer functionalized graphene. Polymer 54, 5087–5103.
Li, D., Muller, M.B., Gilje, S., Kaner, R.B., Wallace, G.G., 2008. Processable aqueous dispersions of graphene nanosheets. Nat. Nanotechnol. 3, 101–105.
Lomeda, J.R., Doyle, C.D., Kosynkin, D.V., Hwang, W.-F., Tour, J.M., 2008. Diazonium functionalization of surfactant-wrapped chemically converted graphene sheets. J. Am. Chem. 130, 16201–16206.
Mungse, H.P., Khatri, O.P., 2014. Chemically functionalized reduced graphene oxide as a novel material for reduction of friction and wear. J. Phys. Chem. 118, 14394–14402.
Novoselov, K.S., Geim, A.K., Morozov, S.V., Jiang, D., Zhang, D., Zhang, Y., Dubonos, S.V., Grigorieva, I.V., Firsov, A.A., 2004. Electric field effect in atomically thin carbon films. Science 306, 666–668.
Paredes, J.I., Villar-Rodil, S., Martinez-Alonso, A., Tascon, J.M.D., 2008. Graphene oxide dispersions in organic solvents. Langmuir 24, 10560–10564.
Pham, V.H., Cuong, T.V., Hur, S.H., Oh, E., Kim, E.J., Shin, E.W., Chung, J.S., 2011. Chemical functionalization of graphene sheets by solvothermal reduction of a graphene oxide suspension in N-methyl-2-pyrrolidone. J. Mater. Chem. 21, 3371.
Rani, S., Kumar, M., Kumar, R., Kumar, D., Sharma, S., Singh, G., 2014. Characterization and dispersibility of improved thermally stable amide functionalized graphene oxide.

Mater. Res. Bull. 60, 143–149.
Remyamol, T., John, H., Gopinath, Pramod, 2013. Synthesis and nonlinear optical properties of reduced graphene oxdie covalently functionalized with polyaniline. Carbon 59, 308–314.
Singh, V., Joung, D., Zhai, L., Das, S., Khondaker, S.I., Seal, S., 2011. Graphene based materials: past, present and future. Prog. Mater. Sci. 56, 1178–1271.
Sobon, G., Sotor, J., Jagiello, J., Kozinski, R., Zdrojek, M., Holdynski, M., Paletko, P., Boguslawski, J., Lipinska, L., Abramsk, K.M., 2012. Graphene Oxide vs. Reduced Graphene Oxide as saturable absorbers for Er-doped passively mode-locked fiber laser. Opt. Express 20, 19463–19473.
Stankovich, S., Dikin, D.A., Piner, R.D., Kohlhaas, K.A., Kleinhammes, A., Jia, Y., Wu, Y., Nguyen, S.T., Ruoff, R.S., 2007. Synthesis of graphene-based nanosheets via chemical reduction of exfoliated graphite oxide. Carbon 45, 1558–1565.
Thakur, S., Karak, N., 2015. Alternative methods and nature-based reagents for the reduction of graphene oxide: a review. Carbon 94, 224–242.
Tran, D.N.H., Kabiri, S., Losic, D., 2014. A green approach for the reduction of graphene oxide nanosheets using non-aromatic amino acids. Carbon 76, 193–202.
Tung, V.C., Allen, M.J., Yang, Y., Kaner, R.B., 2009. High-throughput solution processing of large-scale graphene. Nat. Nanotechnol. 4, 25–29.
Wang, H., Bi, S.-G., Ye, Y.-S., Xue, Y., Xie, X.-L., Mai, Y.-W., 2015. An effective non-covalent grafting approach to functionalize individually dispersed reduced graphene oxide sheets with high grafting density, solubility and electrical conductivity. Nanoscale 7, 35–48.
Wang, A., Yu, W., Huang, Z., Zhou, F., Song, J., Song, Y., Long, L., Cifuentes, M.P., Humphrey, M.G., Zhang, L., Shao, J., Zhang, C., 2016. Covalent functionalization of reduced graphene oxide with porphyrin by means of diazonium chemistry for non-linear optical performance. Sci. Rep. 6, 23325.
Xue, B., Zhu, J., Liu, N., Li, Y., 2015. Facile functionalization of graphene oxide with ethylenediamine as a solid base catalyst for Knoevenagel condensation reaction. Catal. Commun. 64, 105–109.
Yadav, S.K., Yoo, H.J., Cho, J.W., 2012. Click coupled graphene for fabrication of high-performance polymer nanocomposites. Polym. Phys. 10, 23155.
Yoo, M.J., Kim, H.W., Yoo, B.M., Park, H.B., 2014. Highly soluble polyetheramine-functionalized graphene oxide and reduced graphene oxide both in aqueous and non-aqueous solvents. Carbon 75, 149–160.
Zhang, Y., Ma, H.-L., Zhang, Q., Peng, J., Li, J., Zhai, M., Yu, Z.-Z., 2012. Facile synthesis of well-dispersed graphene by γ-ray induced reduction of graphene oxide. J. Mater. Chem. 22, 13064.